Progress In Electromagnetics Research, PIER 40, 131–153, 2003

RADIO PROPAGATION IN RURAL RESIDENTIAL AREAS WITH VEGETATION

N. Blaunstein, D. Censor, and D. Katz

Department of Communication Systems Engineering
Ben Gurion University
P.O. Box 623, Beer-Sheva 84105, Israel

A. Freedman and I. Matityahu

Innowave-ECI, Ltd.
P.O. Box 500, Petah-Tikva 49104, Israel

Abstract—In this paper we describe radio wave propagation within mixed residential area consisting of vegetation and houses. We assume no specific knowledge of the houses and vegetation location, but only of their statistical parameters. A three-dimensional (3D) stochastic approach, which is based on the statistical description of the terrain features, houses and vegetation, and deterministic description of signal decay is presented. The scattering and diffraction from trees and buildings, as well as the diffused reflection from the rough structures of the obstructions are modeled using the statistical description of an array of non-transparent phase screens randomly distributed on the rough terrain. The model, which accounts for single scattering and diffraction phenomena and a similar model, which accounts for multiple scattering effects without effects of diffraction are compared with measurements carried out in typical rural mixed residential areas with vegetation. The accuracy of the theoretical prediction is analyzed accounting possible variations of the terrain features. The approach presented here is applicable in many cases, where specific topographical information is not available.

1. INTRODUCTION

In planning cellular wireless systems it is important to estimate, with a high degree of confidence, the mean signal amplitude decay that would be received by individual subscribers located in various areas surrounding the site of a base station.

Within the built-up areas this problem is complicated by the shadowing effects of tall buildings and other natural and man-made obstructions, and by the so-called channeling phenomena [1–5]. In an urban area the mean signal may differ by 20–30 dB within a traveling ranges of 200–300 m. In suburban areas, one has a better capability to estimate the coverage from a base station since there are relatively few large buildings and channeling effects are less important. In this case, one can assume that the topographic features are predominant.

Vegetation, however, is another significant feature, which affects radio wave propagation in rural areas, but usually it can be neglected in most built-up areas.

Predictions of signal decay in the case of irregular terrain at frequencies less than 500 MHz have been made by a number of authors [6–10] in the end of the fifties to the beginning of the sixties. Usually their estimations are fairly involved and aimed at calculating the loss of point-to-point paths. Later, during the seventies, vegetation and foliage losses have been reported [11–13] at frequencies up to 10 GHz but for relatively few paths. As follows from literature [14–26], trees have both absorbing effect (caused by scattering from foliage) and diffraction effect (caused by a lateral wave created by the top of the tree layer), mainly for propagation over the trees. Up until today, there is not any satisfactory analytical or statistical propagation model, which could explain both building and vegetation effects. Tamir's deterministic model of dielectric layer

is valid only for pure forest environments and for frequencies, which do not exceed 500 MHz [16, 17]. The model developed in [18–21] takes into account the layer of discrete scatterers, as cylinders and disks, which model trees and their branches and leaves, using single-scattering approximation (Born approximation) cannot be converted to the mixed areas containing trees and houses. Models created for rough terrain, including sea surfaces [27–32], cannot be used for forested and built-up areas with complicated profiles of the terrain. At the same time, unified stochastic approach, which sufficiently and fully describes signal power distribution in space domain (for radio coverage prediction) [33–36], in the angle-of-arrival and delay spread domains [36], has limited applications for rural mixed areas, because it deals with such obstructions, as buildings, which are much greater than the wavelength. The results of this approach cannot be automatically converted to scattering from small houses and trees. This is why, following [33–37], we develop a new model, which can be applicable to small obstructions with rough surface where these roughness models the architectural features of houses and branches and leaves of trees (see below).

Below, in Section 2, we present a 3D-statistical model, based on statistical approaches initially constructed for description of radio propagation above the rough terrain [27–31]. Later these methods, developed both for single scattering from rough terrain, based on Kirchhoff approximation (called the "geometrical optic approximation") and for multiple scattering, based on Feynman diagrams (or Green's function expansion), were converted to the built-up rough terrain [32–34]. In [35, 36] this stochastic approach was expanded to the urban and suburban areas, taking into account the buildings' overlay profile and diffraction from buildings' roofs and corners. The next step of investigations was transforming the results obtained for built-up areas to mixed residential areas with vegetation, and creating more adaptive model, which can cover all kinds of the terrain and predict propagation characteristics there. In [38] we presented briefly results of numerical investigations of only one characteristic, the path loss, based on this stochastic approach. The main goal of this work is to describe strictly and informatively our approach to obtain signal decay (or path loss) in the space domain (i.e., spatial attenuation of the signal), accounting to both effects of separate independent scattering of each wave (called "single") from an array of non-transparent trees and houses, and of diffraction from roofs and corners for signal loss effect prediction for UHF/X-band (0.5–10 GHz) propagation. Using the same procedure, as done in [36], we will, in future work, convert the results of our research to investigate signal distribution in the angle-

of-arrival and time delay domains. Section 3 presents a comparison between the proposed 3D-stochastic model using both approaches, with and without diffraction, and the experimental data gathered from a commercial deployment of a Fixed Wireless Access system developed by InnoWave-ECI in a similar area.

The models developed in this work are equivalent to the Hata model [34] in the sense that they are applicable with very little knowledge of the deployment area. However, unlike the Hata model, they use much more information about the area, as will be discussed in Sections 2 and 3. Moreover, comparison between Hata model and the models, similar to above, but developed for urban areas [35–37], has shown that the accuracy of stochastic approach is higher and does not exceed 6–8 dB while the Hata model gives accuracy of 10–15 dB compared to experimental data obtained for different urban and suburban environments. It was shown that the models are useful when specific topographical or morphological information of the deployment area is not known, or cannot be predicted.

2. 3D-STOCHASTIC MODEL OF WAVE SCATTERING IN MIXED AREAS WITH VEGETATION

We propose an approach to investigate the scattering and diffraction effects that accompany the process of radio propagation through rural environment consisting of mixed residential and vegetation areas. This is a combination of probabilistic and deterministic approaches, which describe the random media scattering and diffraction phenomena and follow theoretical concept developed in [27–38]. We use the Kirchhoff (geometrical optic) approximation to account for propagation over a series of houses and trees modeled as absorbing amplitude/phase screens with rough surfaces, which allows us to obtain, from Green's theorem, a solution for the total field scattered from the rough terrain when the scale of each roughness is much higher than the wavelength. Then we use the single and multiple scattering approaches with and without diffraction, respectively, from the non-transparent amplitude/phase screens to obtain the field average intensity attenuation using their real physical parameters, the permittivity and the conductivity, as well as the random distribution of houses and trees structures, the architecture elements, branches and leaves, respectively. We substitute real buildings and trees with rough screens with scales of correlation corresponding to the dimensions of the architectural elements of the buildings or branches and leaves in the case of the trees.

2.1. Model Description

Let us consider a set of houses and trees as blocks and cylinders, respectively, with randomly oriented rough surfaces, which are placed on a flat terrain. According to [34–38], we assume that the reflection properties of the houses and trees are randomly and independently distributed, but they are statistically the same. The values of the reflection coefficient, $R(\varphi_S, \mathbf{r}_S)$, are complex with a uniformly distributed phase on the range $[0, 2\pi]$. In other words, the coefficient of the reflection from the building or tree surface is randomly, but independently, distributed at the obstruction surface. This assumption is often used in real problems of propagation and scattering concerning the rough structures [27–33]. Thus, the average value of the reflection coefficients is zero, i.e., $\langle R(\varphi_s, r_s)\rangle = 0$. Finally, we consider each block or tree as a phase-amplitude screen, the reflection properties of which are described by the complex coefficient of reflection with uniformly distributed phase in the range $[0, 2\pi]$ with correlation scales in the horizontal dimension, ℓ_h, and in the vertical dimension, ℓ_v, respectively. Note, that in built-up areas where buildings' horizontal dimensions are larger than the wavelength, the horizontal reflection properties were not taken into account [33–36]; here we take into account diffused reflection both in horizontal and in vertical planes, which is a new result with respect to those obtained in [33–36].

The geometry of the problem is shown in Fig. 1, where $\mathbf{r}_1$ is the location of the transmitting antenna at the height z_1, $\mathbf{r}_2$ is the location of receiving antenna at the height z_2. Let us derive an average measure of field intensity for waves passing through the mixed layer of houses and trees by use of the single scattering approach taking into account diffraction from tree-tops and building roofs according to [33–38].

2.2. Main Equations

As shown previously in [33–37] for wave propagation through the building layer with randomly distributed buildings (screens), the total field for scattering problem can be presented in the following form:

$$U(\mathbf{r}_2) = U_i(\mathbf{r}_2) + \int_S \left\{ U(\mathbf{r}_S) \frac{\partial G(\mathbf{r}_2, \mathbf{r}_S)}{\partial \mathbf{n}_S} - G(\mathbf{r}_2, \mathbf{r}_S) \frac{\partial U(\mathbf{r}_S)}{\partial \mathbf{n}_S} \right\} dS \quad (1)$$

where $U_i(\mathbf{r}_2)$ is the incident wave field, $G(\mathbf{r}_2, \mathbf{r}_1)$ is the Green's function

$$G(\mathbf{r}_2, \mathbf{r}_1) = \frac{1}{4\pi} \left\{ \frac{\exp[ik|\mathbf{r}_2 - \mathbf{r}_1|]}{|\mathbf{r}_2 - \mathbf{r}_1|} \pm \frac{\exp[ik|\mathbf{r}_2 - \mathbf{r}_1'|}{|\mathbf{r}_2 - \mathbf{r}_1'||} \right\} \quad (2)$$

and $\mathbf{n}_S$ is the vector normal to the terrain surface S at the scattered point $\mathbf{r}_S$. Here $\mathbf{r}_1'$ is the point symmetrical to $\mathbf{r}_1$ relative to the earth

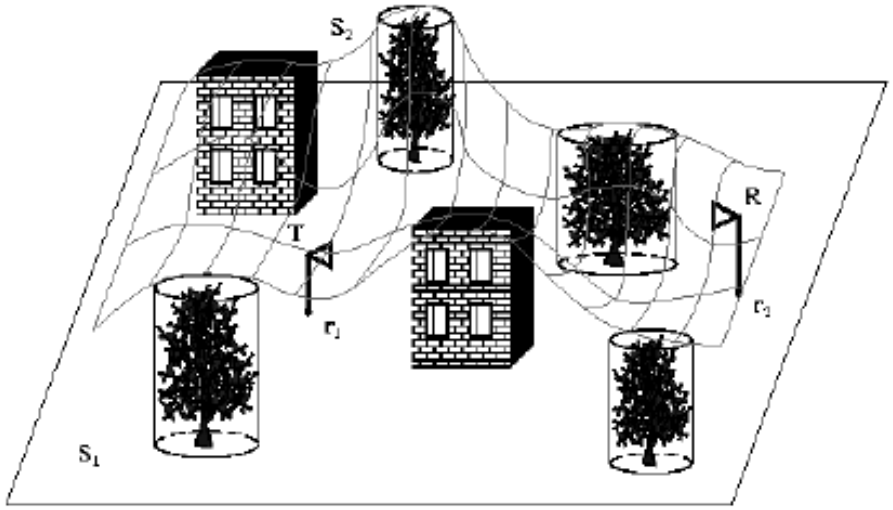

Figure 1. Schematical presentation of the mixed area profile with buildings as blocks and trees as cylinders with rough surfaces randomly distributed on the terrain surrounding the transmitter (T) and receiver (R).

surface S_1; $k = 2\pi/\lambda$ and λ is the wavelength. We consider in the integral of (1) the random surface S (relief of the built-up terrain with vegetation) as the superposition of ideal flat ground surface S_1 and the rough surface S_2 that is created by the tops of the houses or trees. We construct the Green function in such a form (2) to satisfy the electrodynamic approach, e.g., to describe both vertical (sign "+" in (2)) and horizontal (sign "−" in (2)) polarization and corresponding boundary conditions (see details in [33–35]).

Hence if the source is described by formula (2), assuming the surface S_1 as perfectly reflecting, we can exclude the integration over non-disturbed surface S_1, i.e., use the integration only over the disturbed surface S_2, and immediately reduce the scattered field presentation (1) in the following form:

$$U(\mathbf{r}_2) = G(\mathbf{r}_2, \mathbf{r}_1) + \int\limits_{S_2} \left\{ (\mathbf{n}_S \cdot \nabla_S) G(\mathbf{r}_2, \mathbf{r}_S) - G(\mathbf{r}_2, \mathbf{r}_S)(\mathbf{r}_S \cdot \nabla_S) \right\} U(\mathbf{r}_S) dS \tag{3}$$

where $\nabla_S = \left(\frac{\partial}{\partial x_S}, \frac{\partial}{\partial y_S}, \frac{\partial}{\partial z_S}\right)$ and $\mathbf{r}_S$ is the scattered point at the rough terrain.

2.3. The Problem of Single Scattering and Diffraction

Let us, first of all, consider that one of the antennas is higher than the mixed layer average height, $\bar{h}$, i.e., $z_2 > \bar{h} > z_1$, where $\bar{h} = \frac{1}{N}\sum_{i=1}^{N} h_i$, h_i is the height of i^{th} house or tree and N is the number of houses and trees within the area of service. In this case, the field component, which, propagating through such a mixed layer after multiple scattering, is much smaller than that for single scattering [35–38], thus only single-scattering effect should be taken into account.

In this case, using the well-known Kirchhoff (geometrical optics) approximation [27–31], let us determine the single scattered field $U(\mathbf{r}_S)$ from the obstruction layer as the product of the boundary value of the incident wave $U_i(\mathbf{r}_2)$, the reflection coefficient $R(\varphi_S, \mathbf{r}_S)$ and the shadow function $Z(\mathbf{r}_2, \mathbf{r}_1)$, which equals unity, if the scattered point $\mathbf{r}_S$ inside the obstruction layer is simultaneously visible from both antennas placed at points $\mathbf{r}_1$ and $\mathbf{r}_2$ (see Fig. 1), and equals zero in all other cases. Taking that into account, the last formula (3) can be rewritten in case of single scattering as:

$$U(\mathbf{r}_2) = Z(\mathbf{r}_2, \mathbf{r}_1)G(\mathbf{r}_2, \mathbf{r}_1) + 2ik \int_{S_2} \big\{ Z(\mathbf{r}_2, \mathbf{r}_S, \mathbf{r}_1) \cdot R(\varphi_S, \mathbf{r}_S) \cdot \sin\psi_S \cdot G(\mathbf{r}_S, \mathbf{r}_1) \cdot G(\mathbf{r}_2, \mathbf{r}_S) \big\} dS \tag{4}$$

If so, one can present the correlation function of the total field in single-scattering approximation, $K(\mathbf{r}_2, \mathbf{r}_2') = \langle U(\mathbf{r}_2) U^*(\mathbf{r}_2') \rangle$, in the following form, taking into account formula (4):

$$K(\mathbf{r}_2, \mathbf{r}_2') = 4k^2 \Big\langle \int_{S_2} dS_2 \int_{S_2} dS_2' \cdot Z(\mathbf{r}_2, \mathbf{r}_S, \mathbf{r}_1) \cdot Z(\mathbf{r}_2', \mathbf{r}_S', \mathbf{r}_1) \cdot R(\varphi_S, \mathbf{r}_S) \cdot R^*(\varphi_S', \mathbf{r}_S') \cdot \sin\psi_S \cdot \sin\psi_S' \cdot G(\mathbf{r}_2, \mathbf{r}_S) \cdot G(\mathbf{r}_S, \mathbf{r}_1) \cdot G^*(\mathbf{r}_2', \mathbf{r}_S') \cdot G^*(\mathbf{r}_S', \mathbf{r}_1) \Big\rangle \tag{5}$$

To derive the correlation function, $K(\mathbf{r}_2, \mathbf{r}_2')$, we must average the right-hand expression in (5) over the positions of the reflecting surfaces of the obstructions (houses and/or trees), over their number and their reflecting properties. We will do this procedure step by step.

First of all, let us average (5) over the reflection coefficient of each obstruction as a random screen (over the phase interval $[0, 2\pi]$, as the phase distribution of the reflection coefficient), and denote this result by $K_R(\mathbf{r}_2, \mathbf{r}_2')$. Considering now that the correlation scales introduced above are smaller than the obstructions' sizes and the average distances between obstructions, i.e., $\ell_h, \ell_v \ll \bar{h}, \bar{d}, \bar{L}$ but $k\ell_h \gg 1$, $k\ell_v \gg 1$, we can assume that the phase of Green's functions $G(\mathbf{r})$ is changing

approximately linearly. If so, we have

$$K_R(\mathbf{r}_2,\mathbf{r}'_2) = 4k^2 \int_{S_2} dS_2 \int_{S_2} dS'_2 \cdot Z(\mathbf{r}_2,\mathbf{r}_S,\mathbf{r}_1)\cdot Z(\mathbf{r}'_2,\mathbf{r}'_S,\mathbf{r}_1) \cdot \sin^2\psi_S \cdot \langle R(\varphi_S,\mathbf{r}_S)\cdot R^*(\varphi'_S,\mathbf{r}'_S)\rangle \cdot G(\mathbf{r}_2,\mathbf{r}_S)\cdot G(\mathbf{r}_S,\mathbf{r}_1)\cdot G^*(\mathbf{r}'_2,\mathbf{r}'_S)\cdot G^*(\mathbf{r}'_S,\mathbf{r}_1) \tag{6}$$

We also must note that in the integral (5) we consider both points $\mathbf{r}_S$ and $\mathbf{r}'_S$ as simultaneously placed on the surface of the same screen. To obtain $K_R(\mathbf{r}_2,\mathbf{r}'_2)$ let us introduce instead of $\mathbf{r}'_S$ a new variable $\xi = |\mathbf{r}'_S - \mathbf{r}_S|$ and construct at the surface of reflected rough screen the local coordinate system $\{\xi,\eta\}$ with the origin at the point $\mathbf{r}'_S$ with axis 0ξ oriented vertically and axis 0η oriented horizontally. Now, the correlation function for the reflection coefficients can be defined as:

$$\langle R(\varphi_S,\mathbf{r}_S)\cdot R^*(\varphi'_S,\mathbf{r}'_S)\rangle = \Gamma(\varphi_S)\cdot\exp\left\{-\frac{|\xi|}{\ell_v}-\frac{|\eta|}{\ell_h}\right\} \tag{7}$$

where $\Gamma(\varphi_S)$ is the amplitude distribution of the reflection coefficients over the angle φ_S. Let us present (6) using all the approximations above:

$$K_R(\mathbf{r}_2,\mathbf{r}'_2) = 4k^2 \int_{S_2} dS_2 \big[Z_{2S}\cdot Z_{2S'}\cdot\Gamma(\varphi_S)\cdot\sin^2\psi_S \cdot |G_{2S}|^2\cdot|G_{S1}|^2\cdot\exp\{i\mathbf{k}\cdot(\mathbf{r}'_2-\mathbf{r}_2)\}\big] \cdot\int_{-\infty}^{\infty} d\eta\exp\left[-\frac{|\eta|}{\ell_h}+ik\eta(\cos\psi_S-\cos\varphi_S)\right] \cdot\int_{-\infty}^{\infty} d\xi\exp\left[-\frac{|\xi|}{\ell_v}+ik\xi(\sin\theta_2-\sin\theta_1)\right] \tag{8}$$

where for the sake of simplicity we did not write the arguments of each function in the integrand, but only indicated their indexes as a subscripts. Integrating (8) over the variables ξ and η, we finally get

$$K_R(\mathbf{r}_2,\mathbf{r}'_2) = 4k^2 \int_{S_2} dS_2 Z_{2S}\cdot Z_{2S'}\cdot\Gamma(\varphi_S)\cdot\sin^2\psi_S \cdot|G_{2S}|^2\cdot|G_{S1}|^2\cdot\exp\{ik\ell\cos(\varphi-\varphi')\} \cdot\frac{4k\ell_h}{1+(k\ell_h)^2(\cos\psi_s-\cos\varphi_s)^2}\cdot\frac{4k\ell_v}{1+(k\ell_v)^2(\cos\theta_2-\cos\theta_1)^2} \tag{9}$$

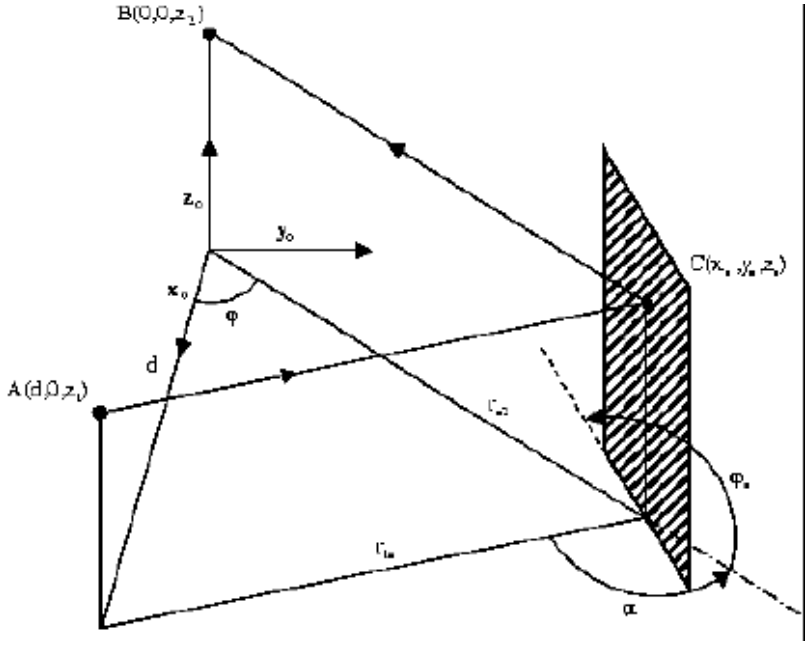

Figure 2. The geometry of single scattering from one of multiple scatterers.

where (see Fig. 2):

$$\ell = |\mathbf{r}_2' - \mathbf{r}_2|,$$

$$\cos\varphi = \left(\frac{\mathbf{r}_2 - \mathbf{r}_1}{|\mathbf{r}_2 - \mathbf{r}_1|} \cdot \frac{\mathbf{r}_2 - \mathbf{r}_S}{|\mathbf{r}_2 - \mathbf{r}_S|}\right), \quad \cos\varphi' = \left(\frac{\mathbf{r}_2 - \mathbf{r}_1}{|\mathbf{r}_2 - \mathbf{r}_1|} \cdot \frac{\mathbf{r}_2 - \mathbf{r}_2'}{|\mathbf{r}_2 - \mathbf{r}_2'|}\right),$$

$$\sin\theta_1 = (z_S - z_1)/|\mathbf{r}_S - \mathbf{r}_1|, \quad \sin\theta_2 = (z_2 - z_S)/|\mathbf{r}_2 - \mathbf{r}_S|$$

Let us note that $d\mathbf{r} = dS_2 \cdot d\mathbf{n}$ is the element of volume V in 3D-space, where $d\mathbf{n}$ is the element of length in the orthogonal direction to the obstruction surface. Then, the averaging (9) over the set of obstructions that are randomly distributed on the ground surface for $k\ell_h \gg 1$, $k\ell_v \gg 1$ gives us [33–36]:

$$K(\mathbf{r}_2, \mathbf{r}_2') = 16\pi \int_V (d\mathbf{r}) \cdot P(\mathbf{r}_1, \mathbf{r}) \cdot \langle\sigma(\mathbf{r}_2, \mathbf{r}, \mathbf{r}_1)\rangle \cdot P_h(z) \cdot P_{BD} \cdot |G(\mathbf{r}_2, \mathbf{r}_S)|^2 |G(\mathbf{r}_S, \mathbf{r}_1)|^2 \cdot \exp\{ik\ell\cos(\varphi - \varphi_0)\} \qquad (10)$$

Here the integration is over the volume V of the mixed layer; $P(\mathbf{r}_1, \mathbf{r})$ is the probability of direct visibility between two points $\mathbf{r}_1$ and $\mathbf{r}$ (i.e.,

that point $\mathbf{r}$ is not shadowed with respect to point $\mathbf{r}_1$) (see Fig. 2):

$$P(\mathbf{r}_1, \mathbf{r}) \equiv P_{12} = \exp\{-\gamma_0 \gamma_{12} |\mathbf{r}_1 - \mathbf{r}|\}, \quad z_2 > z_1 \tag{11}$$

Here

$$\gamma_{12} = (z_2 - z_1)^{-1} \int_{z_1}^{z_2} [P_h(z)][1 - X P_h(z)]^{-1} dz, \tag{12a}$$

and

$$\gamma_0 = 2\bar{d}\nu/\pi \tag{12b}$$

where ν is the density of obstructions in the investigated area per $1\,\mathrm{km}^2$; the parameter γ_0 determines the average horizontal distance of line-of-sight $\bar{\rho}$ (direct visibility), because $\bar{\rho} = \gamma_0^{-1}$; $\bar{d}$ is the average obstruction dimension. Here also the function $\langle \sigma(\mathbf{r}_2', \mathbf{r}, \mathbf{r}_1) \rangle$ is the average differential scattering cross-section from the obstruction [33–36]:

$$\langle \sigma(\mathbf{r}_2', \mathbf{r}, \mathbf{r}_1) \rangle = \frac{\gamma_0 \Gamma(\alpha/2)}{4\pi} \cdot \sin^2 \frac{\alpha}{2} \frac{4k\ell_v}{1 + (k\ell_v)^2 (\cos\theta_2 - \cos\theta_1)^2} \frac{k\ell_h}{1 + (k\ell_h)^2} \tag{13}$$

where α is the angle between vectors $(\mathbf{r}_1 - \mathbf{r}_S)$ and $(\mathbf{r}_2 - \mathbf{r}_S)$ (see Fig. 2).

In the integral (10) the relief function $P_h(z)$ is defined by [33–36]

$$P_h(z) = \int_z^\infty w(h_n) dh_n \tag{14}$$

and determines the probability of the event that all observation points are inside the mixed layer with obstruction heights h_n, $n = 1, 2, 3, \ldots, N$, equally distributed for all numbers n and are not dependent on their total number N. In the integral in (14) the function $w(h_n)$ is the probability density function of the obstruction heights distribution; X in (12a) is the probability of the event, that the projection of each point of observation at the plane $z = 0$, lies inside the contour of any obstruction placed on the plane $z = 0$; $\bar{d}$ is the average dimension of each obstruction. In [35–37] was shown that for built-up areas the buildings' overlay profile is very important characteristics which changes the intensity dependence in the space domain sufficiently depending on the height of both terminal antennas, the transmitter and the receiver, with respect to buildings surrounding them. As was investigated in [38], for mixed residential or rural forested areas, where height of obstructions approximately at the same level,

the built-up terrain profile can be omitted from investigations. In this case $\gamma_{12} = 1$ in (12a) and the probability of LOS between two terminals is simply

$$P_{12} = \exp\{-\gamma_0|\mathbf{r}_1 - \mathbf{r}|\}, \tag{11a}$$

The function P_{BD} in (10) determines the probability of the event, that the wave after being scattered from point $\mathbf{r}$ and after arriving at point $\mathbf{r}_2$ under angle φ will illuminate the horizontal segment ℓ of any obstruction oriented to $(\mathbf{r}_2 - \mathbf{r}_1)$ by angle φ' and is determined as [33–36]:

$$P_{BD} = \exp(-\gamma_0\gamma_{12}|\mathbf{r}'_2 - \mathbf{r}_2|)\exp\{-\nu\varepsilon_{12}r_{12}\ell|\sin\varphi'|\}, \tag{15}$$

where

$$\varepsilon_{12} = (z_2 - z_1)^{-1}\int_{z_1}^{z_2} P_h(z)[1 - XP_h(z)]^{-1}(z - z_1)(z_2 - z_1)^{-1}dz \tag{15a}$$

We must state that formula (9) with all the additional definitions (10)–(15a) fully represents the correlation function in a short-wave approximation (0.9–10 GHz frequency band, which is interesting for the practical cases) and fully describes the single-scattering approximation. From (9) one can easily obtain the expression for average intensity:

$$\begin{aligned}\langle I(\mathbf{r}_2)\rangle &\equiv K(\mathbf{r}_2, \mathbf{r}_2)\\ &= 16\pi\int_V (d\mathbf{r})\cdot P(\mathbf{r}, \mathbf{r}_2)\cdot\langle\sigma(\mathbf{r}_2, \mathbf{r}, \mathbf{r}_1)\rangle\cdot P_h(z)\cdot P_{BD}\\ &\quad\cdot|G(\mathbf{r}_2, \mathbf{r})|^2|G(\mathbf{r}, \mathbf{r}_1)|^2\cdot\exp\{ik\ell\cos(\varphi - \varphi_0)\}\\ &= 4\gamma_0\int_V (d\mathbf{r})\exp\left\{-\gamma_0\left(r + \tilde{r}\frac{\bar{h} - z}{z_2 - z}\right)\right\}\cdot\Gamma\left(\frac{\alpha}{2}\right)\sin^2\frac{\alpha}{2}\\ &\quad\cdot\frac{4k\ell_h|G(\mathbf{r}_2, \mathbf{r})|^2}{1 + (k\ell_h)^2(\cos\psi_s - \cos\varphi_s)^2}\,\frac{4k\ell_v|G(\mathbf{r}, \mathbf{r}_1)|^2}{1 + (k\ell_v)^2(\cos\theta_2 - \cos\theta_1)^2}\end{aligned} \tag{16}$$

Here $r = \sqrt{(x - x_1)^2 + (y - y_1)^2}$, $\tilde{r} = \sqrt{(x_2 - x)^2 + (y_2 - y)^2}$; the integration is over the layer volume $V \equiv \{x, y \in (-\infty, +\infty);\ z \in (0, \bar{h})\}$. Formula (16) is obtained for the case of $0 < z_1 < \bar{h}$, and $z_2 > \bar{h}$. Let us now turn to the cylindrical coordinate system (r, φ, z). Then,

$$x - x_1 = r\cos\varphi, \quad y - y_1 = r\sin\varphi \tag{17}$$

The main contribution to the integral in (16) is given by the area of the layer above the transmitter $r \le \bar{\rho}$ and $(\bar{h} - z) < (z_2 - \bar{h})/(\gamma_0\tilde{r})$ for

which $\tilde{r} = |\mathbf{r}_2 - \mathbf{r}_1|$ and $\gamma_0 \tilde{r} \gg 1$. Far from this region the integrand in (16) attenuates exponentially. This means that the influence of the boundary $z = 0$ at function $G(\mathbf{r}_2, \mathbf{r})$ can be neglected and we can present it for $|\mathbf{r}_2 - \mathbf{r}_1| \gg \bar{\rho}, z_2, \bar{h}$ as:

$$|G(\mathbf{r}_2, \mathbf{r})|^2 \approx \frac{1}{16\pi^2} \frac{1}{|\mathbf{r}_2 - \mathbf{r}_1|} \tag{18}$$

The same is valid for the function $G(\mathbf{r}, \mathbf{r}_1)$:

$$|G(\mathbf{r}, \mathbf{r}_1)|^2 \approx \frac{1}{4\pi^2} \frac{1}{|\mathbf{r} - \mathbf{r}_1|} \sin^2 \left[kz \frac{z_1}{|\mathbf{r} - \mathbf{r}_1|} \right] \tag{19}$$

Finally, after integration (16) over the semi-plane S_B, which consists of virtual sources of diffraction randomly distributed within the mixed layer according to the technique described in [34–36] (see, for example, Section 8.3 and Fig. 8.9 in [34]) and then over variables φ, z, and r, taking into account (18)–(19), we get for $(z_2 - \bar{h})/\bar{h} \gg \gamma_0 d \cdot e^{-\gamma_0 d}$, the following formula of incoherent part of average total signal intensity:

$$\langle I_{inc} \rangle = \frac{\Gamma}{8\pi} \cdot \frac{\lambda \cdot \ell_h}{\lambda^2 + [2\pi \ell_h \gamma_0]^2} \cdot \frac{\lambda \cdot \ell_v}{\lambda^2 + [2\pi \ell_v \gamma_0 (\bar{h} - z_1)]^2} \cdot \frac{\left[(\lambda d / 4\pi^3)^2 + (z_2 - \bar{h})^2 \right]^{1/2}}{d^3} \tag{20}$$

Here $d = |\mathbf{r}_2 - \mathbf{r}_1|$ is the range between two terminal antennas, the transmitter and receiver. This formula is more general than the same expressions for incoherent part of total field obtained in [33–36] for urban propagation, because it accounts for the limit dimensions of obstructions both in vertical and horizontal directions, that is, two-dimensional scattering properties of obstruction surface according to (20). In fact in [33–36] the term $\frac{\lambda \cdot \ell_h}{\lambda^2 + [2\pi \ell_h \gamma_0]^2}$ is absent that changes sufficiently the frequency dependence and dependence on terrain features of scattered field (see (20)). Below, in Section 3, we describe a procedure to estimate the parameters of trees and buildings, such as Γ, ℓ_h, ℓ_v. We estimate them separately and then we estimate the average parameters of obstructions placed within the investigated mixed area.

We must also note that the total average intensity of the field through the mixed layer is the sum of the intensity of the scattering and diffracted wave (20) (incoherent part) and of the intensity of the coherent part $\langle I_{co} \rangle$ created by the wave coming from the source. Taking into account the probability of direct visibility between the source and observation point and using the corresponding formulas (11) and (19)

we obtain for $\langle I_{co} \rangle$ the following expression [34–36]:

$$\langle I_{co} \rangle = \exp\left\{-\gamma_0 d \frac{\bar{h} - z_1}{z_2 - z_1}\right\} \left[\frac{\sin(kz_1 z_2/d)}{2\pi d}\right]^2 \tag{21}$$

Notice again, that formulas (20), (21) were obtained for quasi-homogeneous mixed layer profile with $\gamma_{12} = 1$ from (12a). This assumption is valid for the real situation in the mixed residential areas where the heights of trees and houses are at the same level. As also follows from formulas (20) and (21), they are valid only for the case of an irregular, but not curved, terrain, that is, it is correct for radio links shorter than 15–20 km.

Let us now present results of the model, which describes multiple scattering from an array of obstructions placed on rough terrain without taking into account diffraction phenomena. As was shown in [38], this is actual for scattering from trees in forested environments. We will not repeat all derivations of this model, which is based on presentation of field strength as a set of Green functions and their convolutions. The procedure of these derivations is presented in [34,35] for an array of buildings. Converting the results of the theoretical investigations carried there, we can obtain the following formula for the incoherent part of the total field intensity, taking into account a fact that the mixed layer has quasi-homogeneous profile with approximately the same level of obstructions for the case $\gamma_0 d \gg 1$:

$$\langle I_{inc} \rangle \approx \frac{\gamma_0 \Gamma}{(4\pi)^2} \left[\frac{\Gamma^3}{4(8)^3} \frac{\exp(-\gamma_0 d)}{d} + \frac{\Gamma}{32} \left(\frac{\pi}{2\gamma_0}\right)^{1/2} \frac{\exp(-\gamma_0 d)}{d^{3/2}} + \frac{1}{2\gamma_0} \frac{\exp(-\gamma_0 d)}{d^2}\right] \tag{22}$$

The same procedure as above allow us, following (11) and (19), to obtain for the coherent spectrum of the total field intensity $\langle I_{co} \rangle$ the following expression:

$$\langle I_{co} \rangle = \frac{1}{(4\pi)^2} \frac{\exp(-\gamma_0 \rho)}{\rho^2} \left[2 \sin \frac{k z_1 z_2}{\rho}\right]^2 \tag{23}$$

Then the total field intensity for both models is presented as a sum of the coherent and incoherent parts, i.e.,

$$\langle I_{total} \rangle = \langle I_{co} \rangle + \langle I_{inc} \rangle \tag{24}$$

We use these formulas below to compare it with model of single scattering with diffraction and with experimental data.

3. COMPARISON BETWEEN 3D-STOCHASTIC MODELS AND EXPERIMENTAL DATA

3.1. Description of Experiments

The measurements were performed in commercial deployment of a Fixed Wireless Access (FWA) systems, in three locations in Poland: Lipniki, Koscierzyna and Tarczyn. These are typical rural neighborhoods, with one or two storey buildings surrounded by vegetation. The frequency used was 3.5 GHz. The measurements were made with a transmitter antenna, h_T, of 40 m and 80 m, high above the average tree and building heights while the height of the receiver antenna, h_R, was between 3 to 15 m. Between 5 to 8 points were measured in each of the locations.

The FWA system is a Frequency Hopping system, with 1 MHz instantaneous bandwidth, which is capable of hopping over 80 channels. The antenna used transmission at the base station is a vertically polarized 60 degrees sector antenna with 14 dB gain. The terminal station unit uses a more directive, 18 dB gain antenna, with 10 degrees beam width. The terminal station measures regularly the received strength for all the operating frequencies and provides a minimal, maximal and mean received signal strength values, by request.

The average parameters of the obstructions were estimated in the following manner. For the reflection coefficient, Γ, we used the average value of measure for brick walls and wooden surfaces of trees, that is of 0.3–0.4. As for the correlation scales, ℓ_h and ℓ_v, for trees they are in the order of tens of centimeters, whereas for one-two floor buildings they are in the order of 2–3 meters. In the case of uniformly distributed obstruction we took in our calculations ℓ_h and ℓ_v between 0.5 and 1 meter. The same procedure was used to obtain the minimum, average and maximum obstruction contours density, γ_0. Thus, using the topographic map of the mixed area we divided it to regions of $1\,\mathrm{km}^2$ area each and in each region we estimated the density of the obstructions. In regions with pure vegetation, the parameter γ_0 varies from $\gamma_0 = 0.01\,\mathrm{km}^{-1}$ to $\gamma_0 = 0.1\,\mathrm{km}^{-1}$. In regions where buildings are predominant it ranges between $\gamma_0 = 1\,\mathrm{km}^{-1}$ to $\gamma_0 = 3\,\mathrm{km}^{-1}$. Finally we obtained that the average parameter of obstruction density over the terrain varies between $\gamma_0 = 0.1\,\mathrm{km}^{-1}$ to $\gamma_0 = 1\,\mathrm{km}^{-1}$. These values were used below in the numerical calculations of the path loss for single scattering and diffraction (20)–(21) and multiple scattering without diffraction (22)–(23) problems.

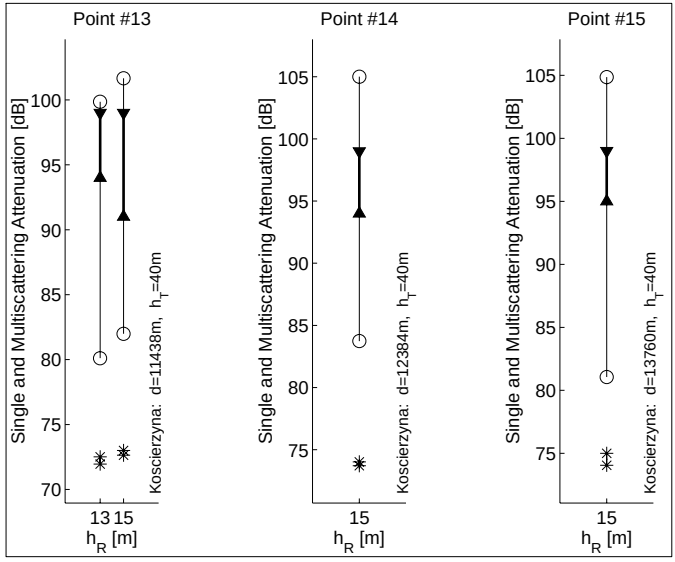

Figure 3. Average total field attenuation versus the height of the receiver for concrete height of 40 m. Wide segment represents experimental data. Circles and asterisks "$*$" represents calculations obtained according to (20)–(21) and (22)–(23), respectively.

3.2. Comparison with Experimental Data

Let us compare the results obtained from the stochastic model, using two approaches: single scattering with diffraction and multiple scattering without diffraction, with the experimental data. We estimate the accuracy of each approach to predict loss characteristics in mixed areas with vegetation by comparison to the measured data. For this purpose we present in Figs. 3–5 the path loss (in dB)

$$L = -10 \log\{(\langle I_{co} \rangle + \langle I_{inc} \rangle)\} \tag{25}$$

as a function of the receiver antenna height calculated according to formulas (20)–(21), (25) for the case of single scattering with diffraction (denoted by circles) and formulas (22)–(25) for the case of multiple scattering without diffraction (denoted by asterisks "$*$"). The experimental data are presented here by a thick line, which connects the minimum and maximum measured values. We also connected the circles and asterisks by thin lines, which span the range between possible results from the minimum value (the bottom circle calculated for $\gamma_0 = 0.1\,\mathrm{km}^{-1}$) and the maximum value (the top circle calculated

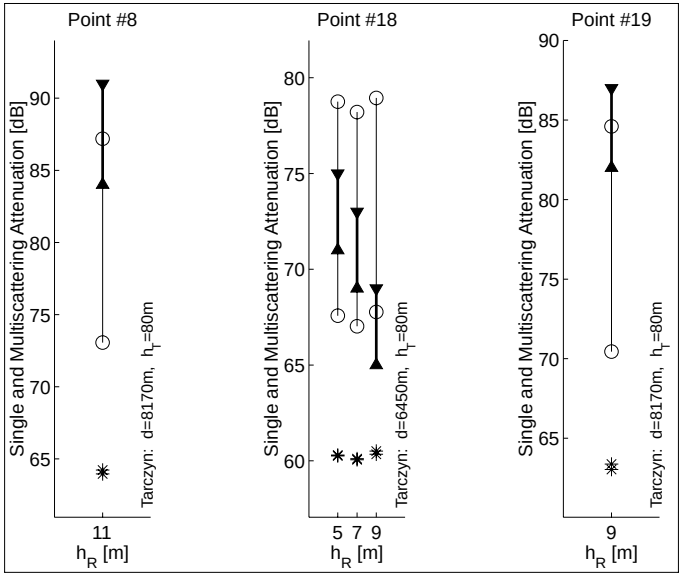

Figure 4. The same, as in Fig. 3, but for the other experimental site, and for transmitter antenna height of 80 m.

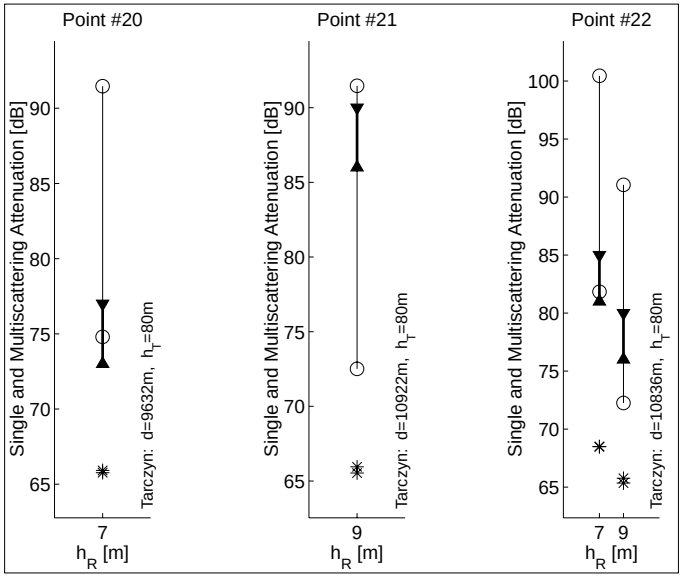

Figure 5. The same, as in Fig. 4, but for the other antenna locations.

for $\gamma_0 = 1\,\mathrm{km}^{-1}$). In the figures the distance d, between the two terminal antennas, the transmitter and receiver, as well as the base station antenna height, h_T, is given in meters. The standard deviation value (STD) and the following prediction error (Err) between two point sets (theory and measurements) were defined as:

$$Err_{model} = R_i - r_i \tag{26}$$

$$\langle Err_{model} \rangle = \frac{1}{N} \sum_{i=1}^{N} (R_i - r_i) \tag{27}$$

$$STD_{model} = \sqrt{\left\langle \left(Err_{model} - \langle Err_{model} \rangle \right)^2 \right\rangle} \tag{28}$$

Here N is the set dimension and R_i and r_i are respectively the theoretically obtained and measured path loss values.

The experimental data were obtained from a commercial deployment does not allow for control of the installation thus it is necessary to present the results from each measurement point separately; conditions of measurements were different for each point of the local experiment. For points 13–14 and 18 the measured data are close to those obtained numerically by use of the model, which takes diffraction into account. The deviation between the calculated and measured values according to (26)–(28) does not exceeds 6–7 dB. On the other hand results of calculations made by use of the model that does not take diffraction into account give much larger deviations from the experimental data, of 8–10 dB (for points 20–22) and of 15–25 dB (for points 14 and 8). The same result can be observed at all sites, as presented in Fig. 4 (for Koscierzyna experimental site) and Fig. 5 (for Tarczyn experimental site), respectively. As follows from the given illustrations, if one uses the statistical model of scattering without diffraction, the difference between the theoretical predictions (denoted in all the figures by asterisks) and the experimental data can exceed 25–30 dB, whereas the same model with diffraction from the obstructions' tops predict the signal intensity attenuation with an accuracy, equivalent to that of the measurement. The deviation between them does not exceed 2–5 dB, an effect, which depends on the density of the obstructions surrounding both terminal antennas, as well as on the antennas' height.

3.3. Sensitivity Analysis

The accuracy of the theoretical prediction depends on the range of variance of each parameter, which describes the terrain features. Thus, as shown in the analysis mentioned above and presented in Figs. 3–5, variations of the tree and house densities, the average height and

reflection properties affect the signal path loss by 10–20 dB. This is why, it is very important to know how accurate should the various parameters be and what is the effect of an error in one of the parameter. Let $\bar{\Theta}$ be a vector of the set of parameters we are using:

$$\bar{\Theta} = \{\Gamma, \gamma_0, l_h, l_v, \delta_1, \delta_2\} \tag{29}$$

and $\Delta\bar{\Theta}$ is a vector of errors in each of those parameters. Here $\delta_1 = (\bar{h} - z_1)$ and $\delta_2 = (z_2 - \bar{h})$. Now, let Θ_i denote one of these parameter, and $\Delta\Theta_i$ be an error in that parameter. It is clear that an error in the path loss introduced by the i^{th} parameter, for other 5 parameters are constant, can be written in the following form:

$$\Delta L_i = \frac{\partial L}{\partial \Theta_i} \Delta\Theta_i \tag{30}$$

Following expression (25) we immediately have from (27) that

$$\frac{\partial L}{\partial \Theta_i} = -\frac{10}{\ln 10} 10^{\frac{L}{10}} \frac{\partial(\langle I\rangle_{co} + \langle I\rangle_{inc})}{\partial \Theta_i} \tag{31}$$

Let us now analyze variations of the total path loss according to (31) for the model of single scattering and diffraction which is stricter than other model of multiple scattering without diffraction describes situation in the mixed environment with vegetation and, as follows from formulas (20) and (21), more sensitive to terrain parameters variations. In this case we get, after some straightforward derivations:

$$\frac{\partial\langle I\rangle}{\partial\Theta_1} \equiv \frac{\partial\langle I\rangle}{\partial\Gamma} = \frac{1}{\Gamma}\langle I\rangle \tag{32a}$$

$$\frac{\partial\langle I\rangle}{\partial\Theta_2} \equiv \frac{\partial\langle I\rangle}{\partial\gamma_0} = -\gamma_0\langle I_{co}\rangle - 2\gamma_0\langle I_{inc}\rangle[K_1 + K_2] \tag{32b}$$

$$\frac{\partial\langle I\rangle}{\partial\Theta_3} \equiv \frac{\partial\langle I\rangle}{\partial l_h} \equiv \frac{\partial\langle I_{inc}\rangle}{\partial l_h} = \langle I_{inc}\rangle K_3 \tag{32c}$$

$$\frac{\partial\langle I\rangle}{\partial\Theta_4} \equiv \frac{\partial\langle I\rangle}{\partial l_v} \equiv \frac{\partial\langle I_{inc}\rangle}{\partial l_v} = \langle I_{inc}\rangle K_4 \tag{32d}$$

$$\frac{\partial\langle I\rangle}{\partial\Theta_5} \equiv \frac{\partial\langle I\rangle}{\partial\delta_1} = \langle I_{inc}\rangle K_5 + \langle I_{co}\rangle K_6 \tag{32e}$$

$$\frac{\partial\langle I\rangle}{\partial\Theta_6} \equiv \frac{\partial\langle I\rangle}{\partial\delta_2} \equiv \frac{\partial\langle I_{inc}\rangle}{\partial\delta_2} = \langle I_{inc}\rangle K_7 \tag{32f}$$

Table 1.

Parameter	Value	Variations	Path Loss Variations
γ_0	0.1–1 km^{-1}	0.05–0.5 km^{-1}	$\pm$(7.0–15.0) dB
Γ	0.6–0.9	0.1–0.3	$\pm$(0.5–1.5) dB
l_h, l_v	0.5–2.0 m	0.1–0.5 m	$\pm$(1.0–3.0) dB
δ_1, δ_2	3–7 m	1–2 m	$\pm$(3.0–5.0) dB

Here

$$K_1 = \frac{(2\pi\ell_h)^2}{\lambda^2 + [2\pi\ell_h\gamma_0]^2}, \qquad K_2 = \frac{[2\pi\ell_v(\bar{h} - z_1)]^2}{\lambda^2 + [2\pi\ell_v\gamma_0(\bar{h} - z_1)]^2}$$

$$K_3 = \frac{1}{\ell_v} - \frac{8\pi^2\gamma_0^2}{\lambda^2 + [2\pi\ell_h\gamma_0]^2}, \qquad K_4 = \frac{1}{\ell_v} - \frac{8\pi^2\gamma_0^2(\bar{h} - z_1)^2}{\lambda^2 + [2\pi\ell_v\gamma_0(\bar{h} - z_1)]^2}$$

$$K_5 = -\frac{4\pi^2\gamma_0^2 l_v^2}{\lambda^2 + [2\pi\ell_h\gamma_0]^2(\bar{h} - z_1)^2}, \qquad K_6 = -\frac{\gamma_0 d}{z_2 - z_1}$$

$$K_7 = \frac{(z_2 - \bar{h})}{\left[(\lambda d/4\pi^3)^2 + (z_2 - \bar{h})^2\right]} \tag{33}$$

Detailed analysis of formulas (31)–(33) for different values of the parameters have shown that variations of all of them, expect the obstructions' density γ_0, weakly influence the deviations of the total path loss of the receiving signal. As described in Table 1, deviations of value of reflection coefficient over the range of $\pm 30\%$ ($\Delta\Gamma = 0.1$–0.3 for $\Gamma = 0.6$–0.9) leads to deviations of the total path loss of $\pm$(0.5–1.5) dB; deviations of the value of the coherence scales over the range of $\pm 30\%$ ($\Delta\ell_h, \Delta\ell_v = 0.1$–$0.5$ m for $\ell_h, \ell_v = 0.5$–2 m) leads to deviations of the total path loss of $\pm$(1.0–3.0) dB; deviations of the value of the difference between antenna heights and the average height of mixed layer over the range of $\pm 30\%$ ($\Delta\delta_1, \Delta\delta_2 = 1$–$2$ m for $\delta_1, \delta_2 = 3$–7 m) leads to deviations of the total path loss of $\pm$(3.0–5.0 dB). Deviations of the parameter γ_0 are at the range of $\pm$(30%–50%) and lead to deviations of the total path loss of $\pm$(7.0–15.0) dB. This result is clearly seen from the results of comparison of the theoretical prediction with the experimental data: a wide coverage of experimental data is observed. This occurs because we have not obtained the precise topographic maps of the tested experimental sites. In any way, the analysis presented above shows that having full information of the area where the communication channels are to be deployed, with the proper

knowledge one can more precisely predict the loss characteristics and finally obtain a full coverage of the areas of service.

4. SUMMARY

We can conclude by saying that the proposed stochastic model, based on the statistical description of different mixed areas with vegetation and their specific distribution and density of obstructions, as well as on the process of diffraction from their tops, provides very good prediction (with error that does not exceed 6–7 dB) of the actual path loss. The accuracy of theoretical prediction according to single scattering model with diffraction is increased with the increase of TX-antenna height.

Results of comparison with different experiments allow us to use the single-scattering approximation with diffraction for mixed residential areas with a good confidence with respect to multi-scattering only for radio traces less than 3–5 km. Moreover one can use the proposed single-scattering approximation with diffraction both for micro- and macro-cellular urban, suburban and rural residential environments for arbitrary heights of both antennas, transmitting and receiving, with respect to the average height of the obstructions.

REFERENCES

1. Blanck, D. M. and D. O. Reudink, "Some characteristics of mobile radio propagation at 836 MHz in the Philadelphia area," *IEEE Trans. Veh. Technol.*, Vol. VT-21, 45–51, May 1972.
2. Bertoni, H. L. and J. Walfisch, "A theoretical model of UHF propagation in urban environment," *IEEE Trans. Antennas Propagat.*, Vol. 36, 1788–1796, Dec. 1988.
3. Blaunstein, N. and M. Levin, "VHF/UHF wave attenuation in a city with regularly spaced buildings," *Radio Sci.*, Vol. 31, No. 2, 313–323, 1996.
4. Blaunstein, N. and M. Levin, "Propagation loss prediction in the urban environment with rectangular grid-plan streets," *Radio Sci.*, Vol. 32, No. 2, 453–467, 1997.
5. Blaunstein, N., "Average field attenuation in the nonregular impedance street waveguide," *IEEE Trans. Anten. and Propag.*, Vol. 46, No. 12, 1782–1789, 1998.
6. Egli, J. J., "Radio propagation above 40 MC over irregular terrain," *Proc. IRE*, Vol. 45, 1383–1391, Oct. 1957.
7. Bullington, K., "Radio propagation fundamentals," *Bell Syst. Tech. J.*, Vol. 36, 593, May 1957.

8. Anderson, L. J. and L. G. Trolese, "Simplified method for computing knife edge diffraction in the shadow region," *IRE Trans. Antennas Propagat.*, Vol. AP-6, 281–286, July 1958.
9. Dougherty, H. T. and L. J. Maloney, "Application of diffraction by convex surfaces to irregular terrain situations," *Radio Phone*, Vol. 68B, 239, Feb. 1964.
10. LaGrone, A. H. and C. W. Chapman, "Some propagation characteristics of high UHF signals in the immediate vicinity of trees," *IRE Trans. Antennas Propagat.*, Vol. AP-9, 957–963, Sept. 1961.
11. Longley, A. G. and R. K. Reasoner, "Comparison of propagation measurements with predicted values in the 20 to 10,000 MHz range," *Environmental Science Services Admin., Tech. Rep.*, ERL 148-ITS 97, Jan. 1970.
12. Reudink, D. O. and M. F. Wazowicz, "Some propagation experiments relating foliage loss and diffraction loss at X-band and UHF frequencies," *IEEE Trans. on Commun.*, Vol. COM-21, 1198–1206, Nov. 1973.
13. Swarup, S. and R. K. Tewari, "Depolarization of radio waves in jungle environment," *IEEE Trans. Antennas Propagat.*, Vol. AP-27, 113–116, Jan. 1979.
14. Tamir, T., "On radio-wave propagation in forest environments," *IEEE Trans. Antennas Propagat.*, Vol. AP-15, 806–817, Nov. 1967.
15. Sachs, D. L. and P. J. Wyatt, "A conducting-slab model for electromagnetic propagation of lateral waves in an inhomogeneous jungle," *Radio Science*, Vol. 3, 125–134, Feb. 1968.
16. Dence, D. and T. Tamir, "Radio loss of lateral waves in forest environments," *Radio Science*, Vol. 4, 307–318, April 1969.
17. Tamir, T., "Radio wave propagation along mixed paths in forest environments," *IEEE Trans. Antennas Propagat.*, Vol. AP-25, 471–477, July 1977.
18. Torrico, S. A. and R. H. Lang, "Bistatic scattering effects from a tree in a vegetated residential environment," *Proc. of National URSI Meeting*, 24–25, Boulder, Colorado, January 5–8, 1998.
19. Torrico, S. A., H. L. Bertoni, and R. H. Lang, "Modeling tree effect on path loss in a residential environment," *IEEE Trans. Anten. Propagat.*, Vol. 46, 107–119, 1998.
20. Twersky, V., "Multiple scattering of electromagnetic waves by arbitrary configurations," *J. Math. Phys.*, Vol. 8, 569–610, 1967.
21. Lang, R. H., "Electromagnetic backscattering from a sparse

distribution of lossy dielectric scatterers," *Radio Sci.*, Vol. 16, 15–30, 1981.

22. Vogel, W. J. and J. Goldhirsch, "Tree attenuation at 869 Mhz derived from remotely piloted aircraft measurements," *IEEE Trans. Anten. and Propagat.*, Vol. AP-34, 1460–1464, 1986.
23. Matzler, C., "Microwave (1–100 GHz) dielectric model of leaves," *IEEE Trans. Geoscience and Remote Sensing*, Vol. 32, 947–949, 1994.
24. Lebherz, M., W. Weisbeck, and K. Krank, "A versatile wave propagation model for the VHF/UHF range considering three dimensional terrain," *IEEE Trans. Antennas Propagat.*, Vol. AP-40, 1121–1131, 1992.
25. Weissberger, M. A., "An initial critical summary of models for predicting the attenuation of radio waves by trees," ESD-TR-81-101, EMC Analysis Center, Annapolis, MD, USA, 1982.
26. Vogel, W. J. and J. Goldhirsch, "Tree attenuation at 869 MHz derived from remotely piloted aircraft measurements," *IEEE Trans. Anten. and Propagat.*, Vol. AP-34, 1460–1464, 1986.
27. Bass, F. G. and I. M. Fuks, *Wave Scattering from Statistically Rough Surfaces*, Pergamon Press, Oxford, 1979.
28. Ishimaru, A., *Electromagnetic Wave Propagation, Radiation, and Scattering*, Prentice-Hall, Englewood Cliffs, NJ, 1991.
29. Charnotskii, M. I. and V. I. Tatarskii, "Tilt-invariant theory of rough-surface scattering: I," *Waves in Random Media*, Vol. 5, No. 4, 361–380, 1995.
30. Tatarskii, V. I. and M. I. Charnotskii, "On the universal behaviour of scattering from a rough surface from small grazing angles," *IEEE Trans. Anten. Propagat.*, Vol. 46, No. 1, 67–72, 1995.
31. Voronovich, A. G., *Wave Scattering from Rough Surfaces*, Springer-Verlag, Berlin, Germany, 1994.
32. Zander, J., "A stochastic model of the urban UHF radio channel," *IEEE Trans. Vehicular Technol.*, Vol. 30, No. 1, 145–155, 1981.
33. Blaunstein, N., D. Katz, D. Censor, A. Freedman, I. Matityahu, and I. Gur-Arie, "Prediction of loss characteristics in built-up areas with various buildings' overlay profiles," *IEEE Antennas Propagation Magazine*, Vol. 43, No. 6, 181–191, 2001.
34. Blaunstein, N., *Radio Propagation in Cellular Network*, Boston-London, 1999.
35. Blaunstein, N., "Prediction of cellular characteristics for various urban environments," *IEEE Antennas Propagation Magazine*, Vol. 41, No. 6, 135–145, 1999.

36. Blaunstein, N., "Distribution of angle-of-arrival and delay from array of buildings placed on rough terrain for various elevations of base station antenna," *J. Communication and Networks*, Vol. 2, No. 4, 305–316, 2000.
37. Blaunstein, N., D. Katz, and D. Censor, "Loss characteristics in urban environment with different buildings' overlay profiles," *Proc. 2001 IEEE Anten. Propag. Int. Symp.*, Vol. 2, 170–173, Boston, Massachusetts, 2001.
38. Blaunstein, N., D. Katz, A. Freedman, and I. Matityahu, "Prediction of loss characteristics in rural and residential areas with vegetation," *Proc. of Int. Conf. on Electromagnetics in Advanced Applications*, 667–670, Torino, Italy, 2001.